Computational and Structural Biotechnology Journal 24 (2024) 12–22

Contents lists available at ScienceDirect

Computational and Structural Biotechnology Journal

journal homepage: www.elsevier.com/locate/csbj

Research Article

Using staged tree models for health data: Investigating invasive fungal infections by aspergillus and other filamentous fungi

Maria Teresa Filigheddu [a], Manuele Leonelli [b,*], Gherardo Varando [c], Miguel Ángel Gómez-Bermejo [d], Sofía Ventura-Díaz [d], Luis Gorospe [d], Jesús Fortún [a,e]

[a] Infectious Diseases Department, Hospital Ramón y Cajal, IRYCIS (Instituto Ramón y Cajal de Investigación Sanitaria); Universidad de Alcalá, Madrid, Spain
[b] School of Science and Technology, IE University, Madrid, Spain
[c] Image Processing Laboratory (IPL), Universitat de València, Valencia, Spain
[d] Radiology Department, Hospital Universitario Ramón y Cajal, Madrid, Spain
[e] Microbiology Department, Hospital Universitario Ramón y Cajal, Madrid, Spain

ARTICLE INFO

Keywords:
Diagnostic criteria
Invasive aspergillosis
Machine learning
Probabilistic graphical models
Staged trees

ABSTRACT

Machine learning models are increasingly used in the medical domain to study the association between risk factors and diseases to support practitioners in understanding health outcomes. In this paper, we showcase the use of machine-learned staged tree models for investigating complex asymmetric dependence structures in health data. Staged trees are a specific class of generative, probabilistic graphical models that formally model asymmetric conditional independence and non-regular sample spaces. An investigation of the risk factors in invasive fungal infections demonstrates the insights staged trees provide to support medical decision-making.

1. Introduction

Risk factors increase an individual's likelihood of negative outcomes for a particular disease or condition. They can range from demographic factors such as age, gender, and ethnicity to behavioral factors such as physical inactivity, smoking, and unhealthy diet. Environmental factors, such as air and water pollution, exposure to radiation, and access to healthcare, also play a role in determining an individual's risk for certain diseases. The study of risk factors and their relationship to medical outcomes is critical in medicine as it can provide insights into the causes of diseases, help identify populations at high risk, and inform the development of prevention and treatment strategies.

Machine learning techniques have emerged as powerful tools for modeling the relationships between risk factors and medical outcomes. These techniques can analyze complex datasets, and identify patterns and relationships that are not immediately apparent. As a result, machine learning has become an essential tool for medical research, helping health practitioners, researchers, and policymakers better understand the impact of risk factors on health outcomes and develop targeted interventions to prevent or mitigate these risks.

Recent trends in applied machine learning focused on developing highly complex and black-box models that lack interpretability and intuitiveness (e.g. [1,57,76]). However, there is an increasing awareness of the criticality of developing AI systems that can provide clear and interpretable explanations for their decision-making process. Explainable AI (XAI) can help address the trust and interpretability issues associated with black-box models and increase users' trust and adoption [2,67].

Probabilistic graphical models [37] are generative machine learning models that visually represent the overall dependence structure using graphs. They do not simply model the conditional distribution of the output of interest given the available risk factors, as in discriminative models, but the overall probability distribution. They thus provide an intuitive platform to perform inferential and independence queries, sensitivity analyses, and risk factors' rankings: all critical activities in applied machine learning modeling [36].

This article showcases the use in medical research of a relatively new class of graphical models called *staged trees* [14,73]. They are probability trees whose inner vertices are colored to embed conditional independence information formally. Recent critical advances have made them a viable, efficient, and highly informative alternative to competitor models in health applications. In particular: (i) software packages now implement staged trees for the use of practitioners in any area of science [12,86]; (ii) faster and more flexible algorithms to learn staged trees from data have been recently developed, scaling them up to dozen of variables (e.g. [15,44,71,72]); (iii) novel visualization frameworks allow for an intuitive depiction of the underlying dependence struc-

* Corresponding author.
E-mail address: manuele.leonelli@ie.edu (M. Leonelli).

https://doi.org/10.1016/j.csbj.2023.11.013
Received 30 July 2023; Received in revised form 7 November 2023; Accepted 7 November 2023
Available online 20 November 2023

ture between the variables [84]; (iv) recent theoretical advances have formalized the use of staged trees for classification problems [13] and causal reasoning and discovery [18,45,80,79].

We showcase the use of staged trees for health data by studying the risk factors associated with invasive fungal infections. Invasive fungal infections by Aspergillus and other filamentous fungi (henceforth called AFF-IFI) have become a critical public health problem in recent decades [8], with an increase in filamentous fungal infections mainly due to Aspergillus spp, and to a lesser extent, Mucor spp and Fusarium spp [41]. AFF-IFIs are significantly related to impaired host immune response, having generally affected patients with hematological malignancies, those undergoing hematopoietic stem cell transplantation, or solid organ transplantation under immunosuppressive treatment [20].

The most widely used diagnostic criteria [20,22] include host factors (mainly immunocompromised conditions), radiological findings (based on angioinvasive signs only, which are partially informative for less immunocompromised patients), and microbiological tests. They have been validated on oncohematological patients with a high level of immunosuppression only. However, an increasing number of patients with impaired immunity from other causes have been observed, with various systemic or bronchopulmonary pathologies (among others, critically ill patients admitted to the intensive care unit (ICU) with severe influenza or other viral infections, repeated use of corticosteroids, poorly controlled diabetes, etc., [42]) with the consequent progressive increase in AFF-IFI in non-oncohematological patients and increased mortality, possibly due to lack of clinical suspicion [52].

Diagnosing these patients is not always easy because the AFF-IFI of non-oncohematological patients differs considerably in the degree of immunosuppression and underlying pathologies. Although they have as a common denominator the development of respiratory forms more frequently with bronchopulmonary expression, they are not always identifiable, unlike oncohematological patients who are more likely to have more evident forms of homogeneous expression [20,22].

The emergent threat of invasive fungal diseases is driven by antifungal resistance and limited global access to diagnostic tools and treatments [10,87]. This menace has vast implications for public health worldwide. It usually leads to more extended hospital stays and treatments, including the need for expensive antifungal medicines, which are often unavailable in developing countries [48,87], Even if fungal infections have been recently recognized as a growing threat to human health worldwide, their study and clinical monitoring received little resources at a global level [8]. This fact hinders our understanding of the problem and makes it impossible to understand its exact burden on public health [87]. In particular, due to its prevalence and expensive treatment, it has become the most expensive fungal disease in the hospital setting [5].

Machine learning techniques for risk prediction and factor identification have only recently started to be used in AFF-IFIs [47,50,89,91]. Only Potter et al. [66] developed a decision support system based on a probabilistic graphical model, namely the Bayesian network model [59], for combat-related AFF-IFI patients. With the present study, we contribute to developing robust and interpretable machine-learning approaches to understanding AFF-IFI diseases.

The two case studies below highlight the critical need to devise new criteria for the timely diagnosis of AFF-IFI patients, more widely applicable than the gold standard EORTC scale [20,22], which must include the overlooked non-conventional group and broncoinvasive patterns, instead of angioinvasive ones only. Further details are given in Section 4 below.

1.1. Health applications

Data-driven algorithms for discovering the genetic causes of various diseases are most commonly based on directed acyclic graphs (DAGs) (e.g. [17,25,65]). Applications of such causal discovery algorithms for understanding clinical risk factors have also recently started to appear [78,85]. Conversely, the use of BNs as a decision-support tool for practitioners and as a platform for the study of risk factors is not as widespread [38–40,51], although recently they have been more frequently used (e.g. [74,75,81]).

Tree-based machine learning algorithms are standard in health, for instance, decision trees [23,35]. However, these are not probability trees formally and highly differ from staged trees. Simple probability (or frequency) trees are vastly used in the health and medical literature [43] and are helpful to practitioners in computing probability queries [7,21]. Staged trees have been used in four medical applications in the past to investigate: type I diabetes [34], the effect of social and economic factors on kids' health [3], COVID-19 trajectories [45], and data missingness patterns in health data [4].

2. Materials and methods

2.1. Data

Retrospectively included in the study were all non-oncohaematological patients diagnosed with proven, probable, or possible pulmonary AFF-IFI according to different diagnostic scales from 1998 to 2021 in 3 hospitals in the Community of Madrid, Spain (Hospital Ramón y Cajal, Hospital Doce de Octubre, Hospital Universitario Fundación Alcorcón) and two hospitals in the metropolitan city of Cagliari, Autonomous Region of Sardinia (Ospedale Santissima Trinitá di Dio and Ospedale Azienda Sanitaria G. Brotzu). The radiological findings were reviewed and described by three radiologists blinded to patients' characteristics.

The chest CT findings and radiological pattern (RP, categorized as angioinvasive or broncoinvasive) of 146 patients[1] with pulmonary AFF-IFI and its prognostic value in non-oncohaematological patients divided into three groups (GR) according to the degree of immunosuppression have been assessed. The first group includes patients with neutropenia not related to haematological diseases (neutropenic group); the second includes patients who do not have neutropenia and have at least one of the following: solid organ transplant and/or tumor, inflammatory/autoimmune diseases, congenital or acquired immunodeficiency, or use of corticosteroids (conventional group); the third includes patients who, in the absence of neutropenia or another "conventional" immunosuppression factor, present alterations in innate and/or adaptive immunity described in the literature as related to specific populations at risk of AFF-IFI (non-conventional group). Despite the known relationship between this last group and AFF-IFI mortality, their risk factors are not included in the most widely used diagnostic scales. Therefore, they are often not diagnosed with AFF-IFI.

A first simpler case study investigates how the two above-mentioned patients' characteristics (radiological pattern and group) are associated with the patients' trajectory as recorded in the hospital: if entered the intensive care unit (ICU), if intubation is performed (INT) and finally the survival outcome (DTH).

In an extended case study, we consider additional risk factors for AFF-IFI that are known to be individually associated with an increase in mortality [28,58]. These are reported in Table 1 together with previous variables.

2.2. Logistic regression

Simple univariate logistic regressions for ICU, INT, and DTH are fitted to data, using as predictor GR, RP, and the preceding variables in the trajectory (ICU → INT → DTH).

To study the relationship between the predictors and their effect on the probability of death, we fitted a group LASSO logistic regression [90], where the regularization parameter was chosen via a 10-fold

[1] The small sample size is due to the limited widespread of AFF-IFI. Related studies include comparable patients' samples if not smaller [49,58].

Table 1
Variables considered for the population under study, acronyms, and sample distributions. Categorical variables are reported as *n* (%). Continuous variables are reported with the median (min-max). The guidelines of Hayes-Larson et al. [32] were followed to construct the table.

	Response sample		Complete case sample		GROUP (GR) - Response sample					
Sample Characteristics	Total (n = 146)		Total (n = 131)		Neutropenic (n = 9)		Conventional (n = 105)		Non-Conventional (n = 32)	
Death (DTH)	55	(38%)	50	(38%)	4	(44%)	35	(33%)	16	(50%)
Intubation (INT)	66	(45%)	62	(47%)	1	(11%)	44	(42%)	21	(66%)
Risk Factors										
CMV Infection (CMV)	33	(23%)	32	(24%)	1	(11%)	30	(29%)	2	(6%)
Diagnostic Time (DT) - days	19	(4-87)	18	(4-87)	10	(4-28)	19	(5-87)	21	(5-59)
Diagnostic Time (DT) - days										
< 16	58	(40%)	54	(41%)	7	(78%)	40	(38%)	11	(34%)
≥ 16	88	(60%)	77	(59%)	2	(22%)	65	(62%)	21	(66%)
ICU	72	(49%)	68	(52%)	2	(22%)	48	(46%)	22	(69%)
Immunotherapy (IM)	86	(59%)	77	(59%)	7	(78%)	79	(75%)	0	(0%)
Malnutrition (MN)	86	(59%)	85	(65%)	5	(56%)	56	(53%)	25	(78%)
Radiological Pattern (RP)										
Angioinvasive	66	(45%)	61	(47%)	8	(89%)	48	(46%)	10	(31%)
Broncoinvasive	80	(55%)	70	(53%)	1	(11%)	57	(54%)	22	(69%)
Systemic Corticoids (SC)	43	(29%)	39	(30%)	1	(11%)	20	(19%)	22	(69%)
Solid Organ Transplant (SOT)	57	(39%)	52	(40%)	2	(22%)	55	(52%)	0	(0%)
Viral Pneumonia (VP)	29	(20%)	28	(21%)	1	(11%)	15	(14%)	13	(41%)
Demographics										
Age - years	65	(14-91)	64	(14-91)	68	(14-87)	63	(17-91)	69	(48-85)
Age - years										
14-60	56	(38%)	55	(42%)	3	(33%)	46	(44%)	7	(22%)
61+	88	(60%)	75	(57%)	6	(67%)	57	(54%)	25	(78%)
NA	2	(2%)	1	(1%)	0	(0%)	2	(2%)	0	(0%)
Male	106	(73%)	96	(73%)	5	(56%)	79	(75%)	22	(69%)

cross-validation. The model also includes as predictors all 2-way interactions, except for ICU:INT to avoid zero counts.

2.3. Bayesian networks

Evolving from the path coefficients method of [88], Bayesian Network (BN) models [59] have become powerful tools in data science and statistics [6,69]. A BN defines a factorization of a random vector's probability mass function (pmf) using a directed acyclic graph (DAG). More formally, let $[p] = \{1, \dots, p\}$ and $\boldsymbol{Y} = (Y_i)_{i\in[p]}$ be a random vector of interest with sample space $\mathbb{Y} = \times_{i\in[p]}\mathbb{Y}_i$. A BN defines the pmf $P(\boldsymbol{Y} = \boldsymbol{y})$, for $\boldsymbol{y} \in \mathbb{Y}$, as a product of simpler conditional pmfs as follows:

$$P(\boldsymbol{Y} = \boldsymbol{y}) = \prod_{i\in[p]} P(Y_i = y_i \mid \boldsymbol{Y}_{\Pi_i} = \boldsymbol{y}_{\Pi_i}), \tag{1}$$

where Π_i are the parents of i in the DAG associated to the BN. Assuming variables are topologically ordered, the BN is further defined by the (symmetric) conditional independence statements $Y_i \perp\!\!\!\perp Y_{[i-1]} | Y_{\Pi_i}$.

The DAG associated with a BN provides an intuitive overview of the relationships between variables of interest. However, it also provides a framework to assess if any generic conditional independence holds for a specific subset of the variables via the so-called d-separation criterion (e.g. [59]). Furthermore, the DAG provides a framework for the efficient propagation of probabilities and evidence via algorithms that take advantage of the structure of the underlying DAG [19].

Although the underlying DAG can be elicited using expert judgment, it is most commonly learned from data using nuanced optimization algorithms (e.g. [29,70]). Moreover, BNs and DAGs are the gold standards for representing and learning causality from data, providing an intuitive framework for defining causal interventions and predicting their effects [29,60,64].

We fit a BN over the same five variables as the logistic regression (GR, RP, ICU, INT and DTH). Since BNs are generative models, they estimate a full probability distribution over all variables, formally modeling their dependence. In particular, a BN is learned using 5000 bootstrap replications of the `tabu` algorithm implemented in `bnlearn` [68], enforcing the causal order GR, RP, ICU, INT, and DTH. Arcs appearing in more than 50% of the replications are retained in the final model.

Similarly in the second case study (Section 3.2) a BN is fitted using the same procedure over all the variables in Table 1 but INT, since it is usually not considered when studying risk factors. Furthermore, the analysis below shows that it is functionally related to ICU and is thus redundant for studying risk factors. Demographic variables are also excluded from the analysis.

2.4. Staged trees

There is an increasing awareness that the stringent assumption of *symmetric* conditional independence of DAGs may be too restrictive in applications [53,63,82]. The most common non-symmetric conditional independence is *context-specific* [9]: the independence between two variables holds only for specific values (called contexts) of conditioning variables: e.g. $Y_i \perp\!\!\!\perp Y_j | Y_k = y_k$ for a specific $y_k \in \mathbb{Y}_k$. More flexible and generic types of independence statements have been defined, namely partial and local [63].

Although models accounting for non-symmetric independence have been defined (e.g. [11,33,54,61,62,77]), staged trees [14,73] are the only ones extensively studied and implemented in user-friendly software [12,86]. Since a formal definition of staged trees is beyond this paper's scope and can be found elsewhere [24,30,84], we introduce them next with an example.

Fig. 1 reports a staged tree over the binary variables radiological pattern (RP), diagnostic time (DT), access to ICU (ICU) and death (DTH). Each root-to-leaf path represents an atomic event (an assignment of all four variables), and inner vertices with corresponding emanating edges are associated with conditional probabilities. For instance, v_1 is associated with the conditional distribution of diagnostic time conditional on an angioinvasive radiological pattern. Colors of the inner vertices are interpreted as equality of conditional distributions: the blue vertices v_1 and v_2 denote that $P(\text{DT} \mid \text{RP} = \text{angio}) = P(\text{DT} \mid \text{RP} = \text{bronco})$, or equivalently DT $\perp\!\!\!\perp$ RP.

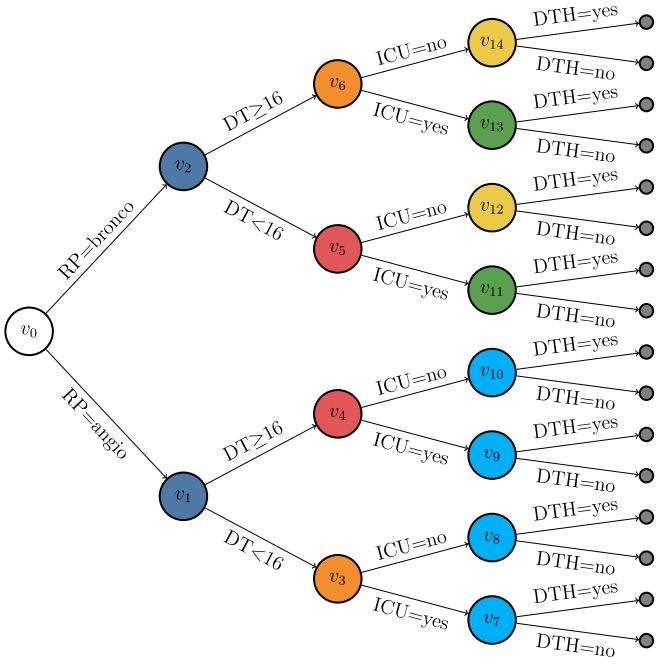

Fig. 1. Example of a staged trees over the variables RP, DT, ICU and DTH.

The flexibility of the coloring allows for asymmetric forms of independence. For instance, the cyan colored vertices $v_7 - v_{10}$ denote the context-specific independence $\text{DTH} \perp\!\!\!\perp \text{ICU}, \text{DT} \mid \text{RP} = \text{angio}$: i.e. conditionally on an angioinvasive radiological pattern, death is independent of both access to ICU and diagnostic time. The yellow and green vertices represent $\text{DTH} \perp\!\!\!\perp \text{DT} \mid \text{ICU}, \text{RP} = \text{bronco}$. Finally, red and orange vertices (at depth 2 from the root) are associated with so-called local independences [63], where no discernable patterns can be identified since they imply equalities $P(\text{ICU} \mid \text{DT} \geq 16, \text{RP} = \text{bronco}) = P(\text{ICU} \mid \text{DT} < 16, \text{RP} = \text{angio})$ and $P(\text{ICU} \mid \text{DT} < 16, \text{RP} = \text{bronco}) = P(\text{ICU} \mid \text{DT} \geq 16, \text{RP} = \text{angio})$. Every BN can be represented exactly as a staged tree [73], while the reverse does not hold since the coloring allows for non-symmetric independence statements that have no graphical representation in a DAG. Although, as for BNs, staged trees could be elicited from experts, they are most often learned from data using heuristic algorithms [12,44].

We employ a staged tree model in the first case study to provide a flexible picture of patients' trajectories and outcomes. A priori, we fix the ordering of the variables as GR, RP, ICU, INT, and DTH to represent the actual steps of the patient's trajectory.

For the extended case study, learning a staged tree over ten binary and one ternary variable is challenging because of the exponentially growing model space size (e.g. [24]). Visualizing the staged tree would also be impossible as it would include $2^{10} \cdot 3 = 3072$ leaves. To circumvent the visualization issue, Varando et al. [84] defined the so-called **minimal DAG**: a DAG representation of the staged tree such that two variables are d-separated in the minimal DAG if and only if the coloring of the staged tree embeds the associated conditional independence.

Because of the high flexibility of the coloring of staged trees, minimal DAGs of staged trees are usually fully connected unless some sparsity is imposed in the structural learning algorithms. Sparsity is the gold standard in Gaussian probabilistic graphical models (e.g. [26]). In the context of discrete BNs, one of the first attempts to impose sparsity was to limit the number of parents each variable can have [27,83]. This makes sense from an applied point of view since, most often, only a limited number of variables can be expected to influence another directly. Setting a maximum number of parents is also available in the standard `bnlearn` software [68].

Limiting the maximum number of parents further decreases the size of the possible models, speeding up structural learning algorithms. For this reason, Leonelli and Varando [44] introduced learning algorithms for k-**parents** staged trees: staged trees whose minimal DAG has a maximum in-degree less or equal to k. Limiting the number of parents has a further advantage in that the probabilities to be estimated are from small dimensional contingency tables, thus providing more reliable estimates with narrower confidence intervals.

3. Results

3.1. 1st case study

We start investigating the effect of the groups' allocation and the radiological pattern on the patient trajectory in the hospital: first, if they enter the ICU; second, if they are intubated; and, ultimately, whether they die.

Table 2 reports the results of the univariate logistic regression analysis, suggesting that access to ICU (OR = 2.26) and intubation (OR = 2.33) are the only two significant predictors of death. Concerning intubation and access to ICU, patients of the non-conventional group have a much higher risk (OR INT = 15.2; OR ICU = 7.70), possibly because they tend to have longer diagnosis times since they are usually not considered at risk of AFF-IFI.

Table 3 reports the estimated ORs from the LASSO logistic regression. Except for RP:INT, all two-way interactions are estimated not to be relevant (OR = 1). Furthermore, as a discriminative model, logistic regression cannot provide additional information about the relationships between risk predictors. Table 4 shows that the predicted probabilities from the LASSO logistic regression, while roughly following the empirical ones from the data, fail to capture the highly non-symmetric relationships between predictors.

Fig. 2 reports the learned BN, which suggests that the group (GR) and the radiological pattern (RP) are independent of the patient's trajectory. Also, access to ICU and intubation are estimated to be independent of survival. This conclusion is possibly due to the strict hypothesis of symmetric independence embedded by BNs. These stringent hypotheses were also confirmed by other classical DAG learning algorithms (e.g. [16,83]).

To have a more comprehensive overview of the patients' trajectories in the hospital, we constructed the data event tree reported in Fig. 3.

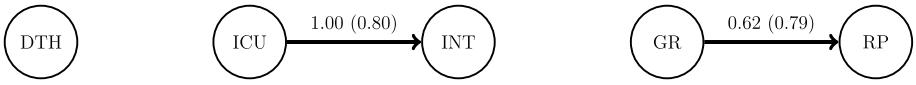

Fig. 2. Structure of the Bayesian network learned over the variables GR, RP, ICU, INT, and DTH. The edge label reports the proportion of times the edge appeared in the bootstrap replications and, in parenthesis, the proportion of times the edge has the given orientation.

Table 2
Odds ratios and 95% confidence intervals for univariate logistic regressions to predict death.

Response	Predictor	Term	OR	CI.Low	CI.High
DTH	GR	Neutropenic (Intercept)	0.80	0.20	3.02
DTH	GR	Conventional	0.63	0.16	2.66
DTH	GR	Non-Conventional	1.25	0.28	5.88
DTH	RP	Bronco. (Intercept)	0.48	0.30	0.76
DTH	RP	Angio.	1.63	0.83	3.21
DTH	ICU	No (Intercept)	0.40	0.23	0.65
DTH	ICU	Yes	2.26	1.15	4.53
DTH	INT	No (Intercept)	0.40	0.24	0.65
DTH	INT	Yes	2.33	1.18	4.67
INT	GR	Neutropenic (Intercept)	0.13	0.01	0.68
INT	GR	Conventional	5.77	1.00	109.0
INT	GR	Non-Conventional	15.2	2.37	302.8
INT	RP	Bronco. (Intercept)	0.95	0.61	1.48
INT	RP	Angio.	0.73	0.37	1.40
INT	ICU	No (Intercept)	0.00	0.00	Inf
INT	ICU	Yes	0.00	0.00	Inf
ICU	GROUP	Neutropenic (Intercept)	0.29	0.04	1.18
ICU	GR	Conventional	2.95	0.67	20.4
ICU	GR	Non-Conventional	7.70	1.54	58.3
ICU	RP	Bronco. (Intercept)	0.95	0.61	1.48
ICU	RP	Angio.	1.05	0.55	2.02

Table 3
Estimated ORs for LASSO logistic regression with 2-way interactions to predict DEATH. Only ORs different from 1 are reported.

Term	OR
Intercept	0.47
GR = conventional	0.84
GR = non-conventional	1.13
RP = angio.	1.20
INT = yes	1.58
RP = angio. & INT = yes	1.33

Even though no machine learning algorithms have been used to learn the staging, the tree is already highly expressive and intuitively shows:

- Which combinations of variables are not observed in the data. These are usually referred to as *observed zeros*. For instance, the only patient in the neutropenic group with a broncoinvasive pattern enters the ICU.
- A non-product sample space. It is known that patients who do not enter the ICU cannot be intubated. For this reason, after the edge ICU = no, the edge INT = no is always the only option. This functional relationship is often called *structural zero*.

The event tree in Fig. 3 is now embellished with a coloring (staging) of its vertices to learn about non-symmetric dependence patterns, which BNs cannot generally represent. The staged tree learned with a hill-climbing greedy algorithm minimizing the BIC [31] using the `stagedtrees` R package [12] is reported in Fig. 4. Table 5 reports the stage probabilities with associated confidence intervals.

Clinically, we observe the following. Patients in the non-conventional and conventional groups are equally likely to have the same radiological pattern (stage 2). In particular, these two groups of patients are more likely to have a broncoinvasive pattern (58%), whereas neutropenic patients are more likely to have an angioinvasive pattern (89%). Admission to the ICU does not depend on the radiological pattern in the case of non-conventional and conventional patients (stages 3 and 4), but admission itself is higher for non-conventional patients (70%). On the other hand, the radiological pattern does affect the probability of admission to the ICU in the case of neutropenic patients. Neutropenic patients with a broncoinvasive pattern have a higher probability (70%) of accessing the ICU than patients with an angioinvasive pattern (43%). Thanks to the colors, we can see that the probability of ICU admission of neutropenic patients with a broncoinvasive pattern and non-conventional patients is the same. The same observation holds for neutropenic patients with an angioinvasive pattern, and conventional patients.

Upon admission to the ICU, patients with a broncoinvasive pattern have a 100% chance of being intubated regardless of the group (stage 5). Patients in the non-conventional and conventional groups are estimated to have the same chance of being intubated (82%), while no neutropenic patients with an angioinvasive pattern are intubated.

Intubated patients with an angioinvasive pattern from the non-conventional and conventional groups have the same estimated chance of dying, which reaches 59% (stage 12). In contrast, the patients with the highest survival (82%) are non-intubated individuals from the non-conventional group with an angioinvasive pattern and ICU admission or conventional patients with a broncoinvasive pattern without ICU admission (stage 10). The second-highest survival probability (73%) is associated with non-intubated patients with an angioinvasive pattern admitted to ICU if in the conventional group or not admitted to the ICU if in the neutropenic group (stage 9). Conventional patients not admitted to the ICU with an angioinvasive pattern have a survival probability of 67%, the same as conventional patients with a broncoinvasive pattern, admitted to the ICU and intubated (stage 11) Patients in the non-conventional group who have not been admitted to the ICU have a survival of 50%, regardless of the radiological pattern (stage 13). Patients in the non-conventional group with a broncoinvasive pattern who have been intubated also have a 50% survival probability (stage 13). The two neutropenic patients admitted to the ICU have died regardless of the radiological pattern and intubation (stage 8).

Despite the small sample size, the staging of the tree has the associated advantage that probabilities are estimated using larger sample sizes than in an event tree. This has a reduction in the uncertainty about the probability estimates as shown in the confidence intervals of Table 5. For instance, it can be noticed that the confidence intervals of the survival probability for patients in stage 10 (highest one) and in stage 12 (lowest non-zero) do not intersect. Of course, this staged tree should me mostly interpreted as an exploratory tool, but the associated uncertainty measures can provide a first indication towards medical evidence.

3.2. Extended case study

The previous case study is highly suited for staged tree modeling since it includes a limited number of variables, with an explicit causal ordering and an asymmetric sample space that the tree can explicitly and intuitively represent. However, recent advances in staged tree theory have made them a viable and efficient tool to investigate dependence in more complex scenarios, including a more extensive array of risk factors, as we showcase in the following data application.

We now consider all risk factors included in Table 1, except for intubation. Observations with missing values were dropped to ensure a fair

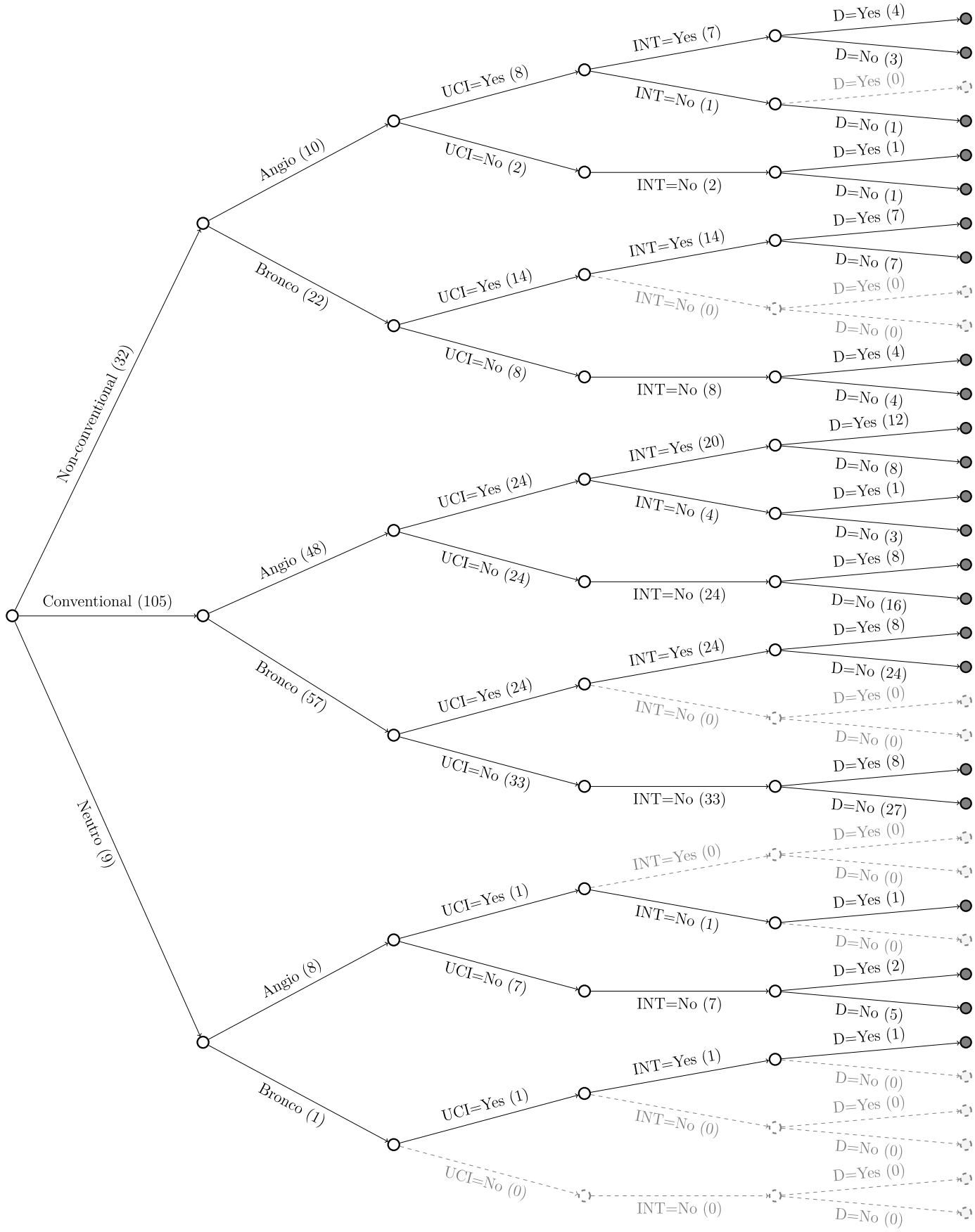

Fig. 3. Event tree over the variables GR, RP, ICU, INT, and DTH (D). The labels of the edges indicate the corresponding events, and in parenthesis, the observation counts along each edge.

Table 4
Empirical and predicted probabilities of death for combinations of significant predictors in the LASSO logistic regression.

		Observed			Predictive		
		GR = neutro	GR = conv.	GR = non-conv.	GR = neutro	GR = conv.	GR = non-conv
PR = angio	INT = yes	NaN	60%	57%	54%	50%	57%
	INT = no	38%	32%	33%	36%	32%	39%
PR = bronco	INT = yes	100%	33%	50%	43%	38%	46%
	INT = no	NaN	18%	50%	32%	28%	35%

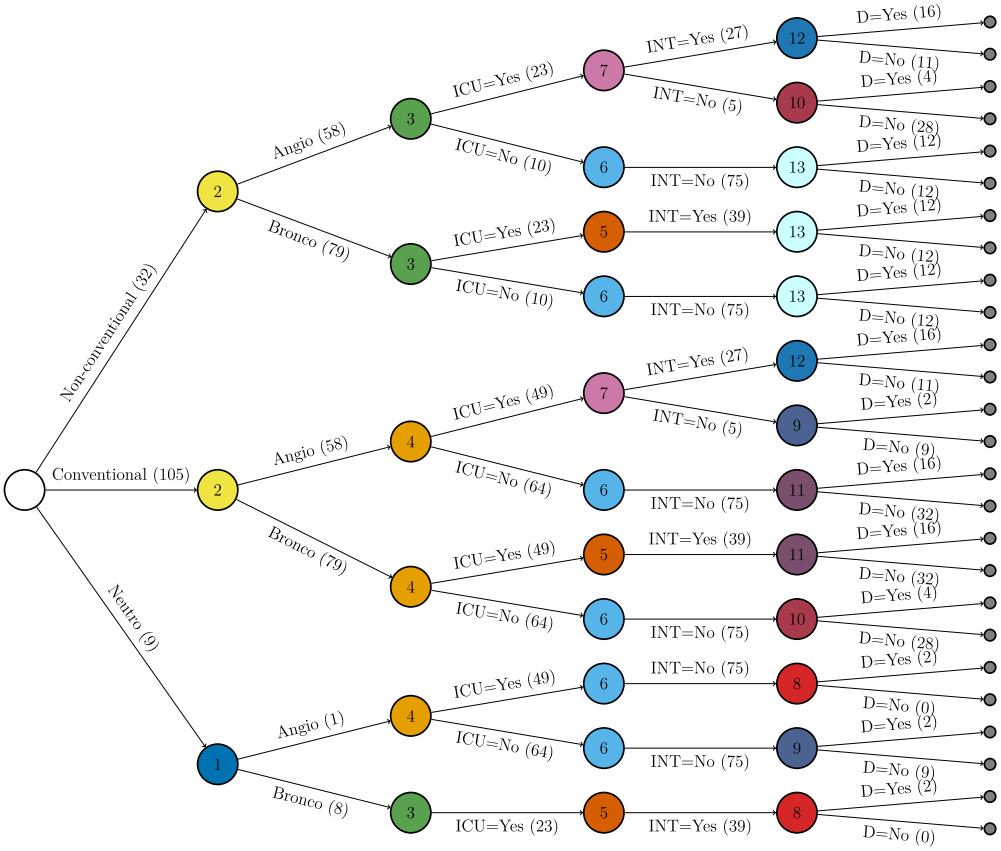

Fig. 4. Staged tree over the variables GR, RP, ICU, INT, and DTH (D). The colors of the nodes denote the stages, the labels of the edges indicate the corresponding events, and in parenthesis the observation counts for each stage.

Table 5
Conditional probability estimates and associated 95% confidence intervals for the staged tree in Fig. 4.

Stage	Probability	Estimate	CI.Low	CI.High	Probability	Estimate	CI.Low	CI.High
1	RP = bronco	0.11	0.00	0.32	RP = angio	0.89	0.68	1.00
2	RP = bronco	0.58	0.49	0.66	RP = angio	0.42	0.34	0.51
3	ICU = yes	0.70	0.54	0.85	ICU = no	0.30	0.15	0.46
4	ICU = yes	0.43	0.34	0.53	ICU = no	0.57	0.47	0.66
5	INT = yes	1.00	1.00	1.00	INT = no	0.00	0.00	0.00
6	INT = yes	0.00	0.00	0.00	INT = no	1.00	1.00	1.00
7	INT = yes	0.84	0.72	0.97	INT = no	0.16	0.03	0.28
8	DTH = yes	1.00	1.00	1.00	DTH = no	0.00	0.00	0.00
9	DTH = yes	0.27	0.01	0.54	DTH = no	0.73	0.46	0.99
10	DTH = yes	0.18	0.05	0.30	DTH = no	0.82	0.70	0.95
11	DTH = yes	0.33	0.20	0.47	DTH = no	0.67	0.53	0.80
12	DTH = yes	0.59	0.40	0.78	DTH = no	0.41	0.22	0.59
13	DTH = yes	0.50	0.30	0.70	DTH = no	0.50	0.30	0.70

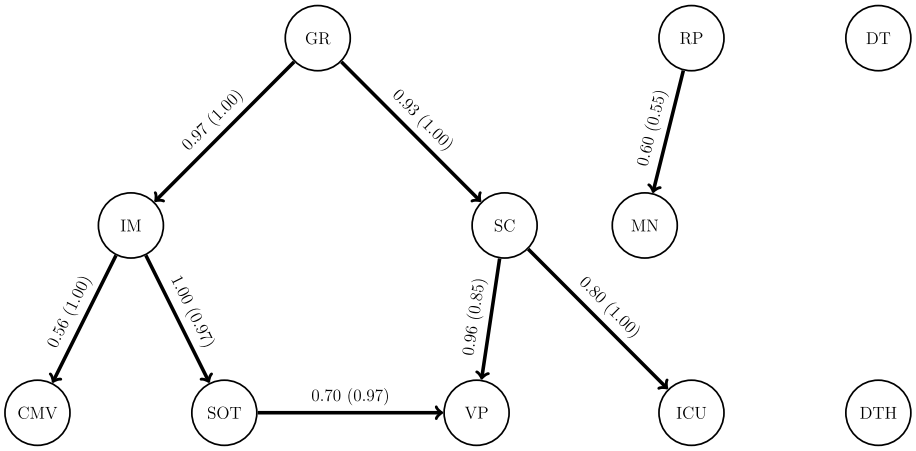

Fig. 5. Structure of the Bayesian network learned over AFF-IFI death-related risk factors. The edge label reports the proportion of times the edge appeared in the bootstrap replications and, in parenthesis, the proportion of times the edge has the given orientation.

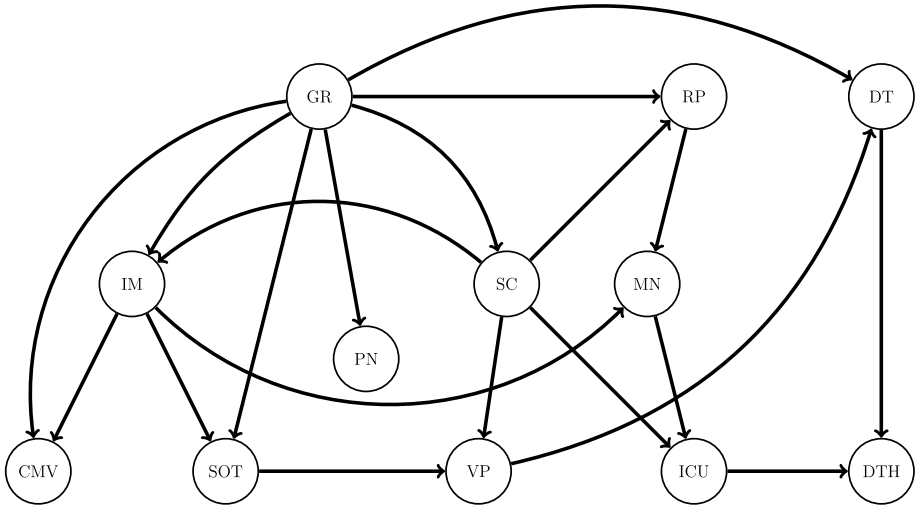

Fig. 6. Minimal DAG associated to learned staged tree over AFF-IFI death-related risk factors.

comparison between BNs and staged trees since the two learning algorithms would tackle this missingness differently. The resulting dataset includes 131 patients, and 80% of the dropped observations were from the conventional group (which included most of the data). Fig. 5 reports the BN learned using the same procedure as in Section 3.1, where edges from death, ICU, and diagnostic time to other variables are forbidden for ease of interpretation. Again death, and in this case also diagnostic time, is independent of all risk factors. This implies, for instance, that angioinvasive and broncoinvasive patients have the same probability of dying. A similar conclusion holds for the patients in the different groups. The BN provides an intuitive representation of the variables' dependence and an efficient platform to answer inferential queries. For instance, the `bnlearn` software can be straightforwardly used to compute the probability that a patient entering the ICU has a solid organ transplant, computed as 0.35. Similarly, we can compute any other probability of interest from the model using software.

Fig. 6 reports the minimal DAG of the 2-parents staged tree over the AFF-IFI death-related risk learned using the algorithm of Leonelli and Varando [46]. We chose two parents to find a balance between the goodness of fit and ease of interpretation. This minimal DAG reveals a much more involved dependence pattern. Diagnostic time, assumed to be marginally independent of death by the BN, directly influences it. Group is a central variable that directly affects diagnostic time, systemic corticoids, radiologica pattern, immunotherapy, solid organ transplant, CMV infection, and viral pneumonia. No variables are assumed to be marginally independent of death.

The 2-parents staged tree better fits the data, having a BIC of 1698, against that of the BN equal to 1749. Given the small dataset, checking predictive accuracy would be unreliable. However, staged trees have been shown to often outperform BNs in predictive tasks [13].

The minimal DAG of the staged tree provides a compressed, partial vision of the staged tree dependence structure. However, such an asymmetric structure is still learned from data. It can be visualized for each variable using a **dependence subtree** [84], reporting the conditional independence coloring of a variable given its parents. Fig. 7 reports the dependence subtree associated with the variable death in the minimal DAG of Fig. 6. It shows that survival is conditionally independent of the diagnostic time given ICU = yes. Patients with a short diagnostic time who do not access the ICU have the smallest probability of death (11%).

The group patients belong to, which has already been observed to be associated with the radiological pattern, has a direct influence on the diagnostic time, which in turn affects mortality. The dependence subtree for the diagnostic time in Fig. 8 shows that non-conventional patients, usually not considered by diagnostic criteria, tend to have a longer diagnostic time. For this reason, the use of new diagnostic criteria that consider the broncoinvasive radiological pattern and a broader classification of risk groups would lead to a rapid diagnosis of AFF-IFI patients, possibly entailing a reduction in mortality. In turn, the use of these criteria would lead to a reduction in hospital pressure in ICU (as

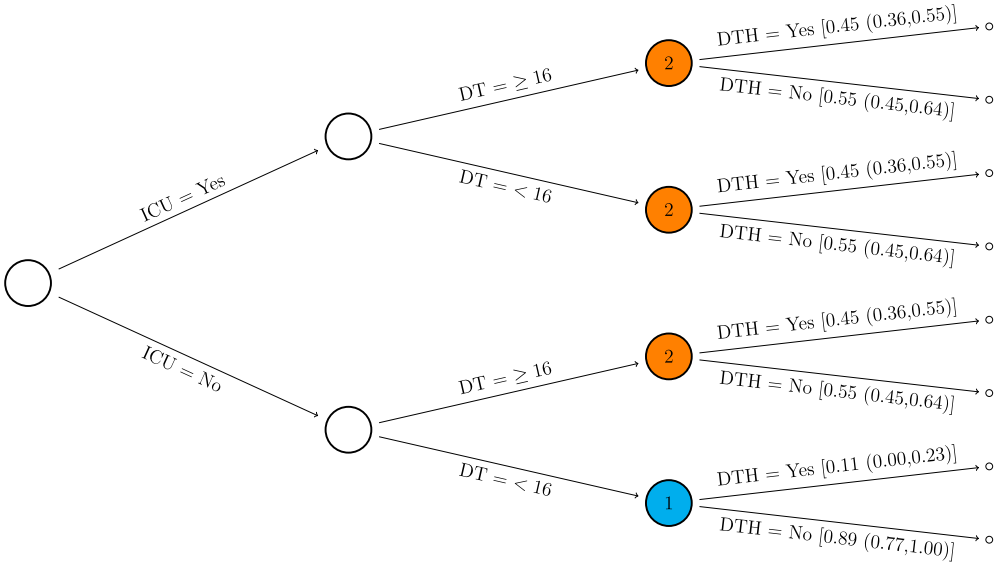

Fig. 7. Dependence subtree for DEATH from the minimal DAG of Fig. 6 with stage probabilities and associated confidence intervals.

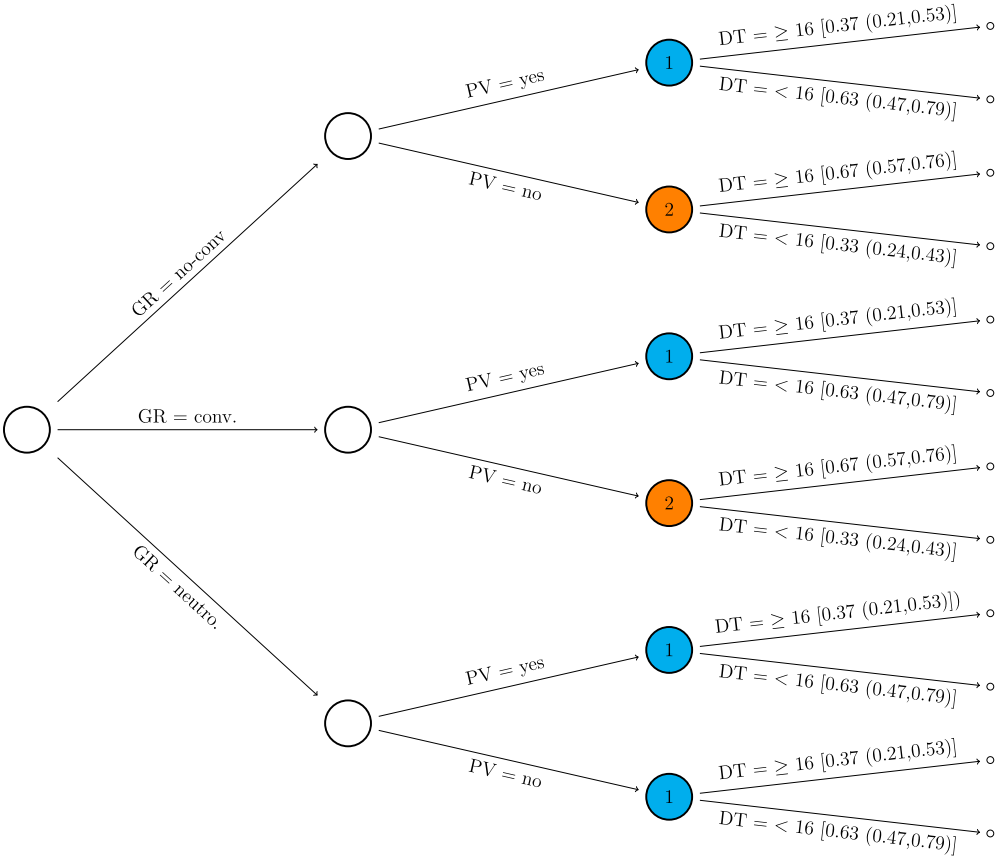

Fig. 8. Dependence subtree for DIAGNOSTIC TIME from the minimal DAG of Fig. 6 with stage probabilities and associated confidence intervals.

observed in case study 1) with a consequent reduction of hospitality costs and an increase in survival [52].

4. Discussion

Observations from the results on the first case study (Section 3.1) reinforce what has been described in the literature, that non-neutropenic patients (conventional and not-conventional) tend to develop respiratory forms more frequently with bronchopulmonary patterns [49,55,56,58], although they differ considerably in the type of underlying diseases and degree of immunosuppression. On the other hand, neutropenic patients more frequently present angioinvasive patterns [20,42].

Regarding actionable conclusions, the observations drawn from the staged tree highlight the need to include information about broncoinvasive patterns in the diagnostic criteria for AFF-IFI since the gold standard EORTC criteria [20,22] completely overlook them. We are currently working on proposing extended diagnostic criteria based on the results of this study. However, their discussion is beyond the scope of this paper.

5. Conclusions

Recently, staged trees have been the focus of research, leading to a better understanding of their underlying dependence structure, more flexible visualization platforms, more efficient data learning algorithms, and open-source implementations. Given all these advances, staged trees can now provide unique insights into data-driven health applications to support practitioners.

Two case studies in AFF-IFIs demonstrated the flexibility of staged trees in intuitively representing highly asymmetric patterns of dependence, which BNs cannot explicitly visualize. Furthermore, given sufficient data, staged trees could be used to answer inferential and independence queries and sensitivity analyses. Using staged trees helped clinicians understand the relationship between risk factors in AFF-IFI more intuitively than BNs.

From a clinical perspective, the analysis showed that the non-conventional group, usually not considered by standard diagnostic scales, shares many characteristics and risks with the neutropenic and conventional groups. Therefore this observation highlights the need to construct more widely applicable entry criteria for diagnostic scales in AFF-IFIs for the timely diagnosis of this group of often overlooked patients. Furthermore, the analysis has shown that the broncoinvasive radiological pattern, not considered within the gold standard diagnostic criteria, plays a critical role in AFF-IFI. Its full clinical appraisal would lead to a timely diagnosis and, consequently, a decrease in mortality.

Despite the small sample size and the lack of statistical validation techniques, all the insights given by staged trees match the clinical intuition of the doctors in our study and information from established literature [49,58]. However, the staged tree provided a more intuitive platform for their interpretation and discussion among clinicians than numerical tables commonly reported in medical studies.

CRediT authorship contribution statement

Maria Teresa Filigheddu: Conceptualization, Data curation, Investigation, Methodology, Validation. **Manuele Leonelli:** Formal analysis, Visualization, Writing – original draft, Writing – review & editing. **Gherardo Varando:** Formal analysis, Visualization, Writing – original draft. **Miguel Ángel Gómez-Bermejo:** Data curation, Investigation. **Sofía Ventura-Díaz:** Data curation, Investigation. **Luis Gorospe:** Data curation, Investigation. **Jesús Fortún:** Resources, Supervision.

Declaration of competing interest

The authors declare that they have no known competing financial interests or personal relationships that could have appeared to influence the work reported in this paper.

References

[1] Alam MZ, Rahman MS, Rahman MS. A random forest based predictor for medical data classification using feature ranking. Inform Med Unlocked 2019;15:100180.
[2] Amiri SS, Mottahedi S, Lee ER, Hoque S. Peeking inside the black-box: explainable machine learning applied to household transportation energy consumption. Comput Environ Urban Syst 2021;88:101647.
[3] Barclay LM, Hutton JL, Smith JQ. Refining a Bayesian network using a chain event graph. Int J Approx Reason 2013;54:1300–9.
[4] Barclay LM, Hutton JL, Smith JQ. Chain event graphs for informed missingness. Bayesian Anal 2014;9:53–76.
[5] Benedict K, Jackson BR, Chiller T, Beer KD. Estimation of direct healthcare costs of fungal diseases in the United States. Clin Infect Dis 2019;68:1791–7.
[6] Bielza C, Larrañaga P. Bayesian networks in neuroscience: a survey. Front Comput Neurosci 2014;8:131.
[7] Binder K, Krauss S, Bruckmaier G, Marienhagen J. Visualizing the Bayesian 2-test case: the effect of tree diagrams on medical decision making. PLoS ONE 2018;13:1–21.
[8] Bongomin F, Gago S, Oladele RO, Denning DW. Global and multi-national prevalence of fungal diseases-estimate precision. J. Fungi 2017;3:57.
[9] Boutilier C, Friedman N, Goldszmidt M, Koller D. Context-specific independence in Bayesian networks. In: Proceedings of the 12th conference on uncertainty in artificial intelligence; 1996. p. 115–23.
[10] Brown GD, Denning DW, Gow NA, Levitz SM, Netea MG, White TC. Hidden killers: human fungal infections. Sci Transl Med 2012;4. 165rv13.
[11] Cano A, Gómez-Olmedo M, Moral S, Pérez-Ariza CB, Salmerón A. Learning recursive probability trees from probabilistic potentials. Int J Approx Reason 2012;53:1367–87.
[12] Carli F, Leonelli M, Riccomagno E, Varando G. The R package stagedtrees for structural learning of stratified staged trees. J Stat Softw 2022;102:1–30.
[13] Carli F, Leonelli M, Varando G. A new class of generative classifiers based on staged tree models. Knowl-Based Syst 2023;268:110488.
[14] Collazo RA, Görgen C, Smith JQ. Chain event graphs. CRC Press; 2018.
[15] Collazo RA, Smith J. A new family of non-local priors for chain event graph model selection. Bayesian Anal 2015;11:1165–201.
[16] Colombo D, Maathuis MH. Order-independent constraint-based causal structure learning. J Mach Learn Res 2014;15:3921–62.
[17] Corander J, Hanage WP, Pensar J. Causal discovery for the microbiome. Lancet Microbe 2022;3:e881–7.
[18] Cowell R, Smith J. Causal discovery through MAP selection of stratified chain event graphs. Electron J Stat 2014;8:965–97.
[19] Cowell RG, Dawid P, Lauritzen SL, Spiegelhalter DJ. Probabilistic networks and expert systems: exact computational methods for Bayesian networks. Springer Science & Business Media; 2007.
[20] De Pauw B, Walsh TJ, Donnelly JP, et al. Revised definitions of invasive fungal disease from the European organization for research and treatment of cancer/invasive fungal infections cooperative group and the national institute of allergy and infectious diseases mycoses study group (EORTC/MSG) consensus group. Clin Infect Dis 2008;46:1813–21.
[21] Detsky AS, Naglie G, Krahn MD, Redelmeier DA, Naimark D. Primer on medical decision analysis: part 2—building a tree. Med Decis Mak 1997;17:126–35.
[22] Donnelly JP, Chen SC, Kauffman CA, Steinbach WJ, et al. Revision and update of the consensus definitions of invasive fungal disease from the European organization for research and treatment of cancer and the mycoses study group education and research consortium. Clin Infect Dis 2020;71:1367–76.
[23] Doupe P, Faghmous J, Basu S. Machine learning for health services researchers. Value Health 2019;22:808–15.
[24] Duarte E, Solus L. Representation of context-specific causal models with observational and interventional data. Available from:. arXiv:2101.09271, 2021.
[25] Foraita R, Friemel J, Günther K, Behrens T, Bullerdiek J, Nimzyk R, et al. Causal discovery of gene regulation with incomplete data. J. R. Stat. Soc., Ser. A 2020;183:1747–75.
[26] Friedman J, Hastie T, Tibshirani R. Sparse inverse covariance estimation with the graphical lasso. Biostatistics 2008;9:432–41.
[27] Friedman N, Nachman I, Pe'er D. Learning Bayesian network structure from massive datasets: the "sparse candidate" algorithm. In: Proceedings of the 15th conference on uncertainty in artificial intelligence; 1999. p. 206–15.
[28] Gioia F, Filigheddu E, Corbella L, Fernández-Ruiz M, López-Medrano F, Pérez-Ayala A, et al. Invasive aspergillosis in solid organ transplantation: diagnostic challenges and differences in outcome in a Spanish national cohort (diaspersot study). Mycoses 2021;64:1334–45.
[29] Glymour C, Zhang K, Spirtes P. Review of causal discovery methods based on graphical models. Front Genet 2019;10:524.
[30] Görgen C, Bigatti A, Riccomagno E, Smith JQ. Discovery of statistical equivalence classes using computer algebra. Int J Approx Reason 2018;95:167–84.
[31] Görgen C, Leonelli M, Marigliano O. The curved exponential family of a staged tree. Electron J Stat 2022;16:2607–20.
[32] Hayes-Larson E, Kezios KL, Mooney SJ, Lovasi G. Who is in this study, anyway? Guidelines for a useful table 1. J Clin Epidemiol 2019;114:125–32.
[33] Jaeger M, Nielsen JD, Silander T. Learning probabilistic decision graphs. Int J Approx Reason 2006;42:84–100.

[34] Keeble C, Thwaites PA, Baxter PD, Barber S, Parslow RC, Law GR. Learning through chain event graphs: the role of maternal factors in childhood type 1 diabetes. Am J Epidemiol 2017;186:1204–8.
[35] Kilic A. Artificial intelligence and machine learning in cardiovascular health care. Ann Thorac Surg 2020;109:1323–9.
[36] Kjaerulff UB, Madsen AL. Bayesian networks and influence diagrams. Springer Science + Business Media; 2008. 200, 114.
[37] Koller D, Friedman N. Probabilistic graphical models: principles and techniques. MIT Press; 2009.
[38] Kyrimi E, Dube K, Fenton N, Fahmi A, Neves MR, Marsh W, et al. Bayesian networks in healthcare: what is preventing their adoption? Artif Intell Med 2021;116:102079.
[39] Kyrimi E, McLachlan S, Dube K, Fenton N. Bayesian networks in healthcare: The chasm between research enthusiasm and clinical adoption. 2020; medRxiv, 2020–06.
[40] Kyrimi E, McLachlan S, Dube K, Neves MR, Fahmi A, Fenton N. A comprehensive scoping review of Bayesian networks in healthcare: past, present and future. Artif Intell Med 2021;117:102108.
[41] Lass-Flörl C. The changing face of epidemiology of invasive fungal disease in Europe. Mycoses 2009;52:197–205.
[42] Latgé JP, Chamilos G. Aspergillus fumigatus and aspergillosis in 2019. Clin Microbiol Rev 2019;33. e00140–18.
[43] Lefrancq N, Paireau J, Hozé N, Courtejoie N, Yazdanpanah Y, Bouadma L, et al. Evolution of outcomes for patients hospitalised during the first 9 months of the SARS-CoV-2 pandemic in France: a retrospective national surveillance data analysis. Lancet Reg Health Eur 2021;5:100087.
[44] Leonelli M, Varando G. Highly efficient structural learning of sparse staged trees. In: International conference on probabilistic graphical models; 2022. p. 193–204.
[45] Leonelli M, Varando G. Context-specific causal discovery for categorical data using staged trees. In: International conference on artificial intelligence and statistics; 2023. p. 8871–88.
[46] Leonelli M, Varando G. Learning and interpreting asymmetry-labeled DAGs: a case study on COVID-19 fear. Available from:. arXiv:2301.00629, 2023.
[47] Li Y, Wu Y, Gao Y, Niu X, Li J, Tang M, et al. Machine-learning based prediction of prognostic risk factors in patients with invasive candidiasis infection and bacterial bloodstream infection: a singled centered retrospective study. BMC Infect Dis 2022;22:1–11.
[48] van der Linden JW, Snelders E, Kampinga GA, Rijnders BJ, Mattsson E, Debets-Ossenkopp YJ, et al. Clinical implications of azole resistance in Aspergillus fumigatus. Emerg Infect Dis 2011;17:1846.
[49] Liu Z, Li Y, Tian X, Liu Q, Li E, Gu X, et al. Airway-invasion-associated pulmonary computed tomography presentations characteristic of invasive pulmonary Aspergillosis in non-immunocompromised adults: a national multicenter retrospective survey in China. Respir Res 2020;21:1–8.
[50] Mayer LM, Strich JR, Kadri SS, Lionakis MS, Evans NG, Prevots DR, et al. Machine learning in infectious disease for risk factor identification and hypothesis generation: proof of concept using invasive candidiasis. In: Open forum infectious diseases; 2022. ofac401.
[51] McLachlan S, Dube K, Hitman GA, Fenton NE, Kyrimi E. Bayesian networks in healthcare: distribution by medical condition. Artif Intell Med 2020;107:101912.
[52] Menzin J, Meyers JL, Friedman M, Perfect JR, Langston AA, Danna RP, et al. Mortality, length of hospitalization, and costs associated with invasive fungal infections in high-risk patients. Am J Health-Syst Pharm 2009;66:1711–7.
[53] Mokhtarian E, Jamshidi F, Etesami J, Kiyavash N. Causal effect identification with context-specific independence relations of control variables. In: International conference on artificial intelligence and statistics, PMLR; 2022. p. 11237–46.
[54] Nicolussi F, Cazzaro M. Context-specific independencies in stratified chain regression graphical models. Bernoulli 2021;27:2091–116.
[55] Nucci M, Nouér SA, Cappone D, Anaissie E. Early diagnosis of invasive pulmonary aspergillosis in hematologic patients: an opportunity to improve the outcome. Haematologica 2013;98:1657.
[56] Nucci M, Nouér SA, Grazziutti M, Kumar NS, Barlogie B, Anaissie E. Probable invasive Aspergillosis without prespecified radiologic findings: proposal for inclusion of a new category of Aspergillosis and implications for studying novel therapies. Clin Infect Dis 2010;51:1273–80.
[57] Painuli D, Bhardwaj S. Recent advancement in cancer diagnosis using machine learning and deep learning techniques: a comprehensive review. Comput Biol Med 2022:105580.
[58] Park S, Kim SH, Choi SH, Sung H, Kim MN, Woo J, et al. Clinical and radiological features of invasive pulmonary aspergillosis in transplant recipients and neutropenic patients. Transplant Infect. Dis 2010;12:309–15.
[59] Pearl J. Probabilistic reasoning in intelligent systems: networks of plausible inference. Morgan Kaufmann; 1988.
[60] Pearl J. Causality. Cambridge University Press; 2009.
[61] Pensar J, Nyman H, Corander J. Structure learning of contextual Markov networks using marginal pseudo-likelihood. Scand J Stat 2017;44:455–79.
[62] Pensar J, Nyman H, Koski T, Corander J. Labeled directed acyclic graphs: a generalization of context-specific independence in directed graphical models. Data Min Knowl Discov 2014;29:503–33.
[63] Pensar J, Nyman H, Lintusaari J, Corander J. The role of local partial independence in learning of Bayesian networks. Int J Approx Reason 2016;69:91–105.
[64] Peters J, Janzing D, Schölkopf B. Elements of causal inference: foundations and learning algorithms. The MIT Press; 2017.
[65] Pingault JB, Richmond R, Smith GD. Causal inference with genetic data: past, present, and future. Cold Spring Harb Perspect Med 2022;12:a041271.
[66] Potter BK, Forsberg JA, Silvius E, Wagner M, Khatri V, Schobel SA, et al. Combat-related invasive fungal infections: development of a clinically applicable clinical decision support system for early risk stratification. Mil Med 2019;184:e235–42.
[67] Ribeiro MT, Singh S, Guestrin C. "Why should I trust you?": Explaining the predictions of any classifier. In: Knowledge discovery and data mining (KDD); 2016.
[68] Scutari M. Learning Bayesian networks with the bnlearn R package. J Stat Softw 2010;35:1–22.
[69] Scutari M, Denis JB. Bayesian networks: with examples in R. CRC Press; 2021.
[70] Scutari M, Graafland CE, Gutiérrez JM. Who learns better Bayesian network structures: accuracy and speed of structure learning algorithms. Int J Approx Reason 2019;115:235–53.
[71] Shenvi A, Liverani S. Beyond conjugacy for chain event graph model selection. Available from:. arXiv:2211.03427, 2022.
[72] Silander T, Leong TY. A dynamic programming algorithm for learning chain event graphs. In: Proceedings of the 16th international conference in discovery science. Springer; 2013. p. 201–16.
[73] Smith JQ, Anderson PE. Conditional independence and chain event graphs. Artif Intell 2008;172:42–68.
[74] Song W, Qin Z, Hu X, Han H, Li A, Zhou X, et al. Using Bayesian networks with Tabu-search algorithm to explore risk factors for hyperhomocysteinemia. Sci Rep 2023;13:1610.
[75] van der Stap L, van Haaften MF, van Marrewijk EF, de Heij AH, Jansen PL, Burgers JM, et al. The feasibility of a Bayesian network model to assess the probability of simultaneous symptoms in patients with advanced cancer. Sci Rep 2022;12:22295.
[76] Sun F, Sun J, Zhao Q. A deep learning method for predicting metabolite–disease associations via graph neural network. Brief Bioinform 2022;23:bbac266.
[77] Talvitie T, Eggeling R, Koivisto M. Learning Bayesian networks with local structure, mixed variables, and exact algorithms. Int J Approx Reason 2019;115:69–95.
[78] Tennant PW, Murray EJ, Arnold KF, Berrie L, Fox MP, Gadd SC, et al. Use of directed acyclic graphs (DAGs) to identify confounders in applied health research: review and recommendations. Int J Epidemiol 2021;50:620–32.
[79] Thwaites P. Causal identifiability via chain event graphs. Artif Intell 2013;195:291–315.
[80] Thwaites P, Smith JQ, Riccomagno E. Causal analysis with chain event graphs. Artif Intell 2010;174:889–909.
[81] Tian T, Kong F, Yang R, Long X, Chen L, Li M, et al. A Bayesian network model for prediction of low or failed fertilization in assisted reproductive technology based on a large clinical real-world data. Reprod Biol Endocrinol 2023;21:1–12.
[82] Tikka S, Hyttinen A, Karvanen J. Identifying causal effects via context-specific independence relations. Adv Neural Inf Process Syst 2019;32.
[83] Tsamardinos I, Brown LE, Aliferis CF. The max-min hill-climbing Bayesian network structure learning algorithm. Mach Learn 2006;65:31–78.
[84] Varando G, Carli F, Leonelli M. Staged trees and asymmetry-labeled DAGs. Available from:. arXiv:2108.01994, 2021.
[85] Velikova M, van Scheltinga JT, Lucas PJ, Spaanderman M. Exploiting causal functional relationships in Bayesian network modelling for personalised healthcare. Int J Approx Reason 2014;55:59–73.
[86] Walley G, Shenvi A, Strong P, Kobalczyk K. cegpy: modelling with chain event graphs in Python. Knowl-Based Syst 2023;274:110615.
[87] World Health Organization. WHO fungal priority pathogens list to guide research, development and public health action. 2022.
[88] Wright S. The method of path coefficients. Ann Math Stat 1934;5:161–215.
[89] Yan C, Hao P, Wu G, Lin J, Xu J, Zhang T, et al. Machine learning-based combined nomogram for predicting the risk of pulmonary invasive fungal infection in severely immunocompromised patients. Ann Transl Med 2022;10.
[90] Yang Y, Zou H. A fast unified algorithm for solving group-lasso penalize learning problems. Stat Comput 2015;25:1129–41.
[91] Yuan S, Sun Y, Xiao X, Long Y, He H. Using machine learning algorithms to predict candidaemia in ICU patients with new-onset systemic inflammatory response syndrome. Front Med 2021;8:720926.